Negative Thermal Expansion in the Siliceous Zeolites Chabazite and ITQ-4: A Neutron Powder Diffraction Study

David A. Woodcock and Philip Lightfoot*

School of Chemistry, University of St. Andrews, North Haugh, St. Andrews, Fife, KY16 9ST, United Kingdom

Luis A. Villaescusa, Maria-Jose Díaz-Cabañas, and Miguel A. Camblor

Instituto de Tecnología Química, Avda. Los Naranjos s/n, 46071 Valencia, Spain

Dennis Engberg

The ISIS Facility, CLRC Rutherford Appleton Laboratory, Chilton, Didcot, Oxfordshire, OX11 OQX, United Kingdom

Received April 12, 1999. Revised Manuscript Received June 14, 1999

We present the results of quantitative variable-temperature neutron powder diffraction experiments performed on the OSIRIS instrument at the ISIS facility on the pure silica zeolites chabazite and ITQ-4. Chabazite has been found to be one of the most strongly contracting materials known, with a linear expansion coefficient $\alpha_v/3$ varying from -0.5×10^{-6} to -16.7×10^{-6} K^{-1} over the temperature range 293−873 K. Full Rietveld refinement has been carried out using three different refinement strategies: free isotropic refinements, refinement using geometrical restraints, and a rigid body refinement. The free isotropic refinement was found to be the most successful. In agreement with previous studies on ZrW_2O_8 and $Sc_2(WO_4)_3$ type materials, we suggest that changes in Si−O−Si interpolyhedral bond angles are the driving force for the contraction mechanism. ITQ-4 has also been found to contract over the temperature range 95−510 K, with $\alpha_v/3$ varying from -2.2×10^{-6} to -3.7×10^{-6} K^{-1} over this range.

Introduction

Microporous materials such as the pure silica zeolites ITQ-1, ITQ-3, and SSZ-23,[1] faujasite,[2] ZSM-5,[3] and the aluminophosphates AlPO-5[3] and AlPO-17[4] are among the most recent additions to the ever growing number of materials known to contract on heating. Computer simulations too, such as those by Tschaufeser et al.[5] and Gale[6] have played their part in identifying new materials exhibiting this unusual property. One of the most significant points to arise from both the experimental and computational work is the suggestion that in all these framework structures, the thermal behavior may be described in terms of dynamic rocking of essentially rigid polyhedra. This approximation has been borne out in powder diffraction studies of the system $Sc_2(WO_4)_3$[7]and the only two zeolitic systems so far analyzed quantitatively—SiO_2 (faujasite)[2] and AlPO-17.[4] Within both faujasite and AlPO-17 the mechanism of contraction is believed to be due to the transverse vibrations of the two coordinate bridging oxygens.

Our own previous studies on members of the $NaZr_2(PO_4)_3$ (NZP) family suggest that it may be relevant in some cases to consider a certain degree of flexibility of the polyhedra.[8,9] In this paper, we continue our studies of the mechanism of negative thermal expansion in pure SiO_2 zeolites, and present results of powder neutron diffraction data analysis on two polymorphs, chabazite (CHA) and ITQ-4 (IFR). In the case of chabazite, we describe and compare three different Rietveld refinement strategies, viz., free isotropic refinement, geometrically restrained refinement and isotropic rigid body refinement. This type of analysis should in principle help discriminate between dynamic and static effects. Neither of the two previously studied systems, faujasite and AlPO-17, showed a systematic change in atomic coordinates with temperature, implying that harmonic transverse vibrations of the bridging oxygen atoms were responsible for the thermal contraction, rather than genuine static change in Si−O−Si or O−Si−O bond angles. One of the main characteristics

(1) Woodcock, D. A.; Lightfoot, P.; Wright, P. A.; Villaescusa, L. A.; Díaz-Cabañas, M.-J.; Camblor, M. A. *J. Mater. Chem.* **1999**, *9*, 349−351.
(2) Attfield, M. P.; Sleight, A. W. *Chem. Commun.* **1998**, 601.
(3) Park, S. H.; Grosse Kunstleve, R. W.; Graetsch, H.; Gies, H. *Stud. Surf. Sci. Catal.* **1997**, *105*, 1989.
(4) Attfield, M. P.; Sleight, A. W. *Chem. Mater.* **1998**, *10*, 2013.
(5) Tschaufeser, P.; Parker, S. C. *J. Phys. Chem.* **1995**, *99*, 10609.
(6) Gale, J. D. *J. Phys. Chem. B* **1998**, *102*, 5423−5431.
(7) Evans, J. S. O.; Mary, T. A.; Sleight, A. W. *J. Solid State Chem.* **1998**, *137*, 148.
(8) Woodcock, D. A.; Lightfoot, P.; Ritter, C. *Chem. Commun.* **1998**, 107.
(9) Lightfoot, P.; Woodcock, D. A.; Jorgensen, J. D.; Short, S. *J. Inorg. Mater.* **1999**, *1*, 53.

10.1021/cm991047q CCC: $18.00
Published on Web 08/31/1999

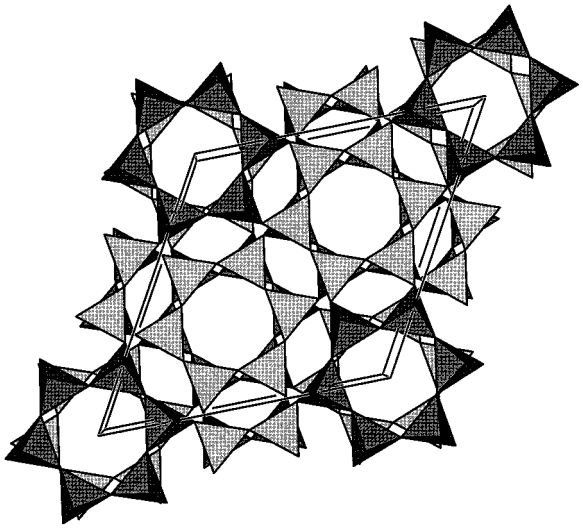

Figure 1. Polyhedral representation of the structure of chabazite viewed down the *c* axis.

of the thermal contraction in $Sc_2(WO_4)_3$[7] and ZrW_2O_8,[10] however, is a change in bridging angles (M−O−M′).

The structure of chabazite is similar to that of AlPO-17 in that both are composed of systematic stacking of double six rings as shown in Figure 1. Within chabazite the rings are stacked in the sequence AABBCC, whereas in AlPO-17 they are stacked AABAAC (ERI structure type). This results in similar hexagonal lattice parameters for the two structures, similar framework densities and both having six- and eight-membered ring channels.

IFR materials (termed as ITQ-4 or SSZ-42[11]) have been modeled by Gale.[6] His results predict negative thermal expansion along all cell axes and an increase in the monoclinic angle, leading to an overall volume contraction.

The overall mechanism of negative thermal expansion in zeolites remains unclear. Studies by Dove et al.[12] have outlined a Rigid Unit Mode theory of negative thermal expansion which states that the existence of low-energy distortions can be predicted depending on the connectivities of the tetrahedra. Contraction of the material is dependent on the flexibility of the M−O−M bridging angle which is in turn dependent on these low-energy distortions. It has also been suggested by Sleight[4] that an empirical way of predicting which zeolites and aluminophosphates contract is to compare the cell volumes of the as-prepared and calcined−dehydrated materials. If the as-prepared volume is lower than the calcined volume, then the framework has contracted around the structure-directing agent, and therefore has the ability to contract and may exhibit negative thermal expansion.

Experimental Section

Pure silica samples of chabazite and ITQ-4 were prepared by the methods outlined in the literature[13,14] by Camblor et al. Each sample was initially studied by variable-temperature X-ray powder diffraction on a STOE STADI-P diffractometer. Data quality was sufficient to quantify the behavior of unit cell parameters vs temperature. Both had a reduction in cell volume over the temperature range room temperature to 773 K.

Table 1. Results from Profile Fit for Chabazite

temperature, K	merit	unrestrained	soft constraints	rigid body
293	χ^2	5.840	5.874	6.684
293	R_{wp}	0.0385	0.0385	0.0411
293	R_p	0.0484	0.0484	0.0535
473	χ^2	7.043	7.227	7.951
473	R_{wp}	0.0626	0.0630	0.0666
473	R_p	0.0639	0.0631	0.0661
673	χ^2	1.808	1.864	2.207
673	R_{wp}	0.0552	0.0554	0.0610
673	R_p	0.0522	0.0610	0.0558
773	χ^2	2.265	2.332	2.533
773	R_{wp}	0.0610	0.0613	0.0645
773	R_p	0.0601	0.0601	0.0627
873	χ^2	1.970	2.073	2.269
873	R_{wp}	0.0567	0.0573	0.0609
873	R_p	0.0495	0.0492	0.0522

The sample of chabazite was placed in a vanadium can and run in furnace RALF3 on the OSIRIS instrument[15] at the ISIS facility at the CCLRC Rutherford Appleton Laboratory. The choppers were run at 25 Hz, giving with the current opening angles, a bandwidth of 4 Å for each setting. To have overlap between the different measurements six different settings were used to cover the range 2−16 Å. This gives in the near backscattering geometry of OSIRIS a d-spacing range of about 1.0−7.0 Å. Measurements were recorded at 293, 473, 673, 773, 873, and 1073 K. A measurement of an empty can was recorded and subtracted from the initial data before starting refinements. The first of the chabazite refinements to be carried out using the GSAS program[16] was completely unrestrained, refining unit cell parameters, scale factor, background, peak shape (Gaussian double exponential), atomic coordinates, and isotropic temperature factors, which were constrained by atom type. Each refinement consisted of refinements of 28 variables, 274 reflections over the range 1.0−7.0 Å. The experiment was repeated firstly using soft constraints for Si−O (1.61 ± 0.005) and O−O (2.58 ± 0.005) distances and secondly by treating the SiO_4 tetrahedra as rigid bodies, with Si−O fixed at 1.61 Å, and isotropic thermal parameters for Si and O.

The sample of ITQ-4 was run in the cryofurnace at temperatures 95, 142, 225, 342, 442, and 510 K. Choppers were set as for chabazite giving the same d-spacing range of 1.0−7.0 Å. As above, the background was subtracted and a free isotropic refinement performed. Due to the increased complexity of this structure we feel that a full quantitative discussion is not appropriate.

Results

Chabazite R_{wp}, R_p, and χ^2 values for unrestrained, restrained, and rigid body refinements are shown in Table 1. The Rietveld fit at 293 K is shown in Figure 2.

(10) Evans, J. S. O.; Mary, T. A.; Vogt, T.; Subramanian, M. A.; Sleight, A. W. *Chem. Mater.* **1996**, *8*, 2809.
(11) Chen, C. Y.; Finger, L. W.; Medrud, R. C.; Crozier, P. A.; Chan, I. Y.; Harris, T. V.; Jones, S. I. *J. Chem. Soc., Chem. Commun.* **1997**, 1775.
(12) Pryde, A. K. A.; Hammonds, K. D.; Dove, M. T.; Heine, V.; Gale, J. D.; Warren, M. C. *J. Phys. Condens. Matter.* **1996**, *8*, 10973.
(13) Diaz-Cabanas, M. J.; Barrett, P. A.; Camblor, M. A. *Chem. Commun.* **1998**, *17*, 1881.
(14) Barrett, P. A.; Camblor, M. A.; Corma, A.; Jones, R. H.; Villaescusa, L. A. *J. Phys. Chem. B* **1998**, *102* (21), 4147.
(15) Martin, D.; Engberg, D. *Physica B*, in press.
(16) Larson, A. C.; Von Dreele, R. B. Los Alamos National Laboratory Report No. LA-UR-86-748, 1987.

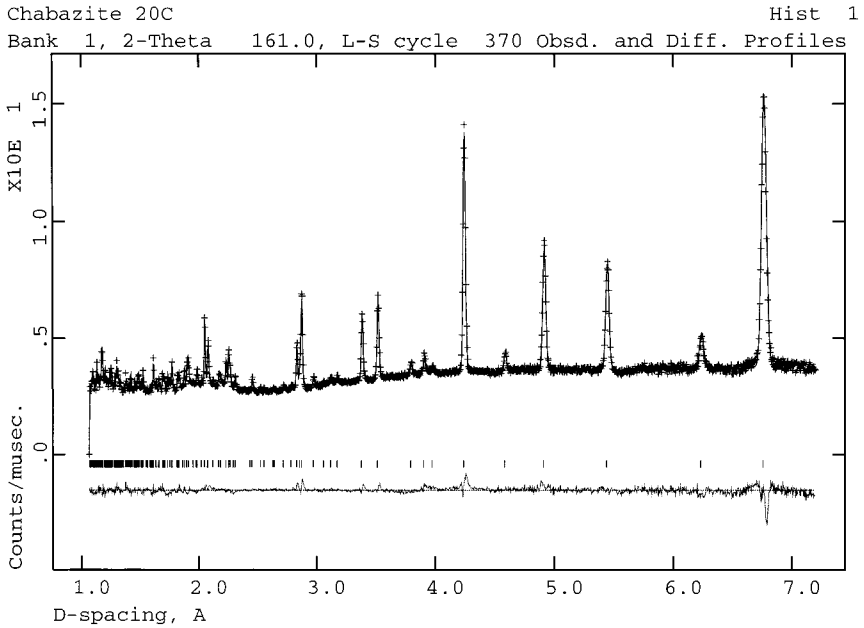

Figure 2. Typical neutron Rietveld plot for chabazite at 293 K.

Table 2. Experimentally Determined Atomic Coordinates for Chabazite at 293 and 873 K

space group = $R\bar{3}m$										
T = 293 K						T = 873 K				
a = 13.5252(3) Å, c = 14.7342(5) Å, V = 2334.3(1) Å^3						a = 13.4661(4) Å, c = 14.6395(6) Å, V = 2299.0(1) Å^3				
	x	y	z	$U_{iso} \times 100$ Å^2	multiplicity		x	y	z	$U_{iso} \times 100$ Å^2	multiplicity
Si	0.2275(4)	0.0009(5)	0.1030(3)	3.5(2)	36i	Si	0. 2287(5)	0.0034(5)	0.0988(4)	3.6(2)	36i
O1	0.1188(2)	−0.1188(2)	0.1299(3)	−0.17(6)	18h	O1	0.1204(2)	−0.1204(2)	0.1314(3)	1.94(8)	18h
O2	0.3333	0.0213(3)	0.1667	−0.17(6)	18g	O2	0.3333	0.0209(3)	0.1667	1.94(8)	18g
O3	0.1962(4)	0.0981(2)	0.1206(3)	−0.17(6)	18h	O3	0.1964(4)	0.0982(2)	0.1195(3)	1.94(8)	18h
O4	0.2592(3)	0	0	−0.17(6)	18f	O4	0.2615(3)	0	0	1.94(8)	18f

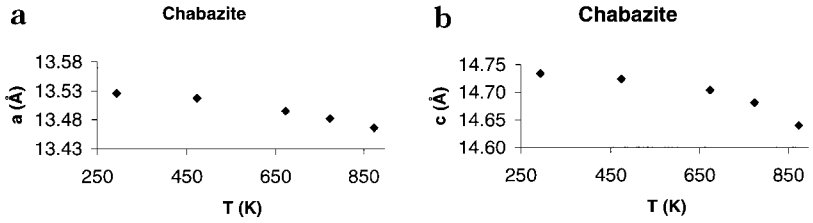

Figure 3. Plots of the evolution of unit cell parameters vs temperature for chabazite for (a) the *a* axis and (b) the *c* axis.

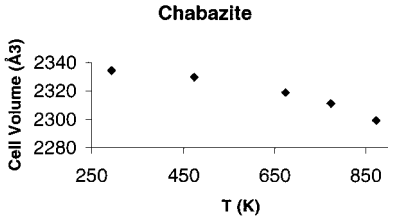

Figure 4. Plot of the evolution of unit cell volume vs temperature for chabazite.

From these results, we are confident that the free refinement strategy is optimal. Most significantly, the isotropic rigid body model is clearly inferior and therefore invalid. Due to limited data, we are unable to carry out a full TLS rigid body refinement so cannot test the suggestions of Evans and Sleight.[7]

The unit cell parameters and atomic coordinates at the highest and lowest temperatures are shown in Table 2. Plots of the behavior of unit cell parameters and volume are shown in Figures 3 and 4. As can be seen, the behavior of all parameters is nonlinear. Polynomial coefficients of thermal expansion were therefore calculated using the following:

Table 3. Experimentally Determined Polynomial Parameters for Chabazite

axis	p_2	p_1	p
a	-1.200×10^{-7}	-2.833×10^{-5}	13.526
c	-3.553×10^{-7}	6.862×10^{-5}	14.73
vol	-9.670×10^{-5}	7.587×10^{-4}	2334

$$p = p_2T^2 + p_1T + p_o \quad (1)$$

$$\alpha = \frac{p_1 + 2p_2T}{p} \quad (2)$$

The resulting values are tabulated in Table 3. The chabazite results from T = 1073 K have not been considered in this calculation as the fit was starting to deteriorate due to a splitting of some reflections, suggesting a decomposition or a transformation to lower symmetry.

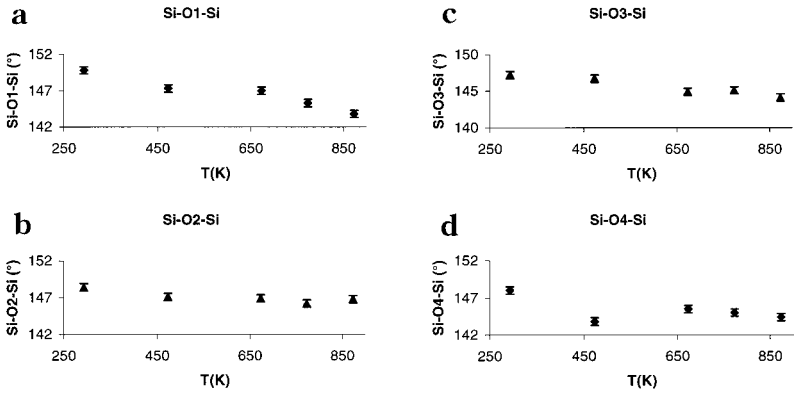

Figure 5. Thermal evolution of the Si−O−Si tetrahedral angles in chabazite: (a) Si−O1−Si, (b) Si−O2−Si, (c) Si−O3−Si, and (d) Si−O4−Si.

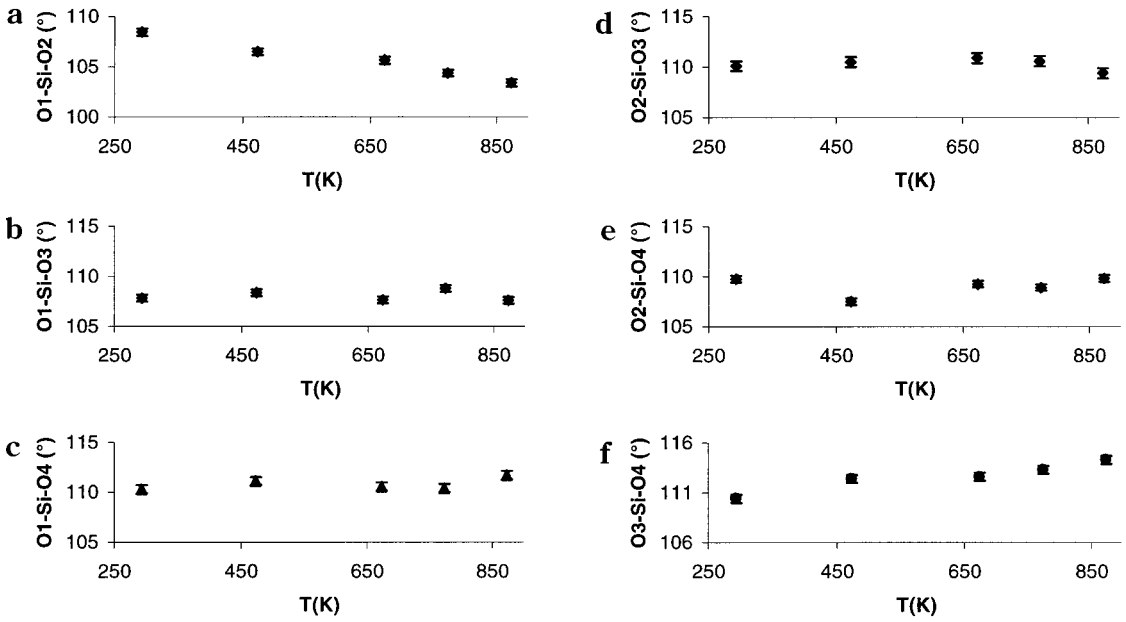

Figure 6. Thermal evolution of the O−Si−O bridging angles in chabazite: (a) O1−Si−O2, (b) O1−Si−O3, (c) O1−Si1−O4, (d) O2−Si−O3, (e) O2−Si−O4, and (f) O3−Si−O4.

Considering the structural parameters, the Si−O−Si and O−Si−O angles are the parameters which show the greatest change. They are plotted in Figures 5 and 6. There is a strong contraction in the Si−O1−Si angle and in the Si−O3−Si angle. This, coupled with the expansion in the Si−O1 bond length (Figure 7) which forms part of the same single six-ring configuration, suggests a narrowing of the channels as the Si's move closer together. A representation of this single six-membered ring viewed down the *c* axis is shown in Figure 8. The contraction of the ring is clearly responsible for the contraction of the *a* and *b* axes.

There is an expansion of the O3−Si−O4 angle and a contraction of the O1−Si−O2 angle which form opposite sides of the same tetrahedron. It is perhaps this distortion in particular which is responsible for the failure of the rigid body model in this case as the tetrahedra can no longer be treated as rigid.

The double six-membered ring structure viewed perpendicular to the *c* axis is shown in Figure 9. The bridging Si−O4−Si angle can be clearly seen. There is a small decrease in this angle, and an apparent shortening of the Si−O4 distance. This may be an artifact of the isotropic refinement strategy and may really reflect increased transverse motion of O4. However the combined effect is to pull the layers closer together, as revealed in the corresponding Si−Si distance (Figure 7d) and shorten the *c* axis.

The Rietveld fit for ITQ-4 at 95 K is shown in Figure 10. Behavior of unit cell parameters is shown in Figure 11 and their polynomial fits are given in Table 4. Full Rietveld refinements, using the soft constraints model, were carried out at each temperature. These confirmed that the expected model in *I*2/*m* is valid throughout the temperature range studied. However the data are not of high enough quality to identify the key structural trends influencing the behavior. One significant feature in contrast to previous simulations of ITQ-4 (SSZ-42)[6] is that we have found an expansion of the *c* axis and a contraction of the monoclinic angle (Table 5).

The hypothesis relating an expansion of the unit cell volume on calcination to negative thermal expansion is inconclusive in the case of ITQ-4 (Figure 12), which expands by only 0.06% upon calcination and is not borne out at all in the case of chabazite which contracts by 0.18% on calcination. A given zeolite may be prepared with different structure-directing agents in such a way that removal of the template may cause expansion or

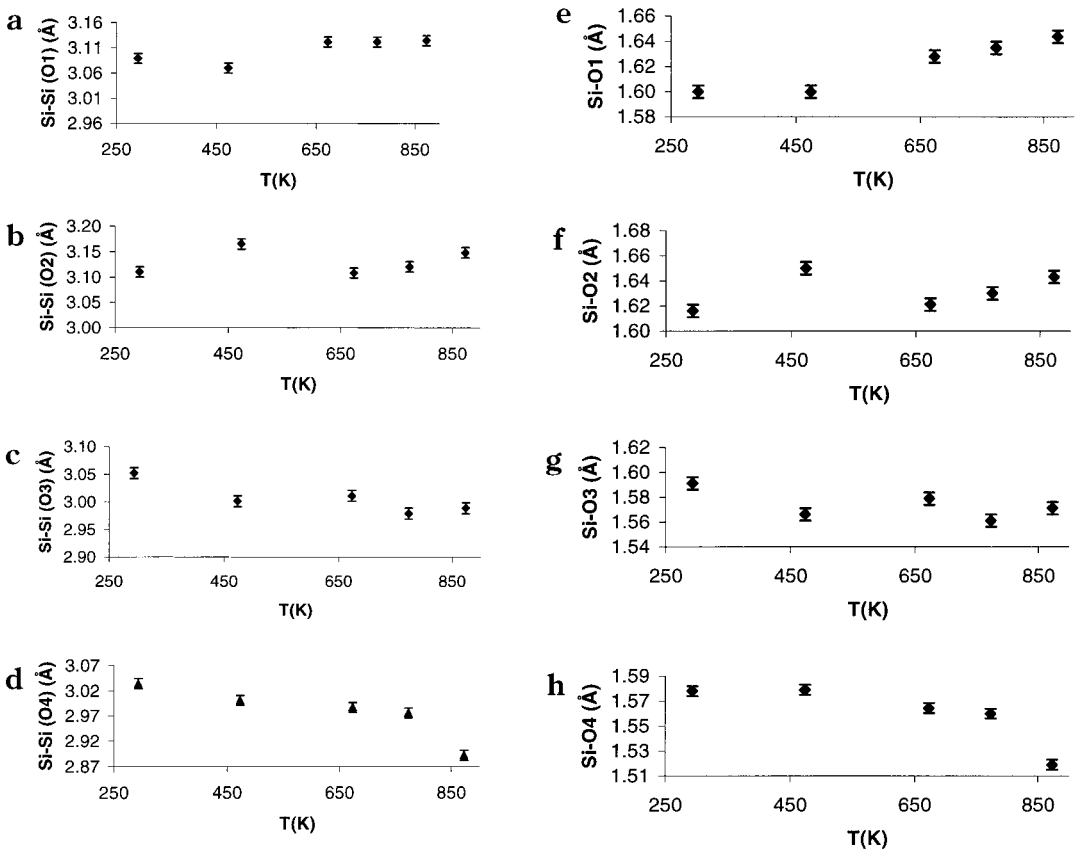

Figure 7. Thermal evolution of the Si−Si nonbonding and Si−O bond distances in chabazite: (a) Si−Si (O1), (b) Si−Si (O2), (c) Si−Si (O3), (d) Si−Si (O4), (e) Si−O1, (f) Si−O2, (g) Si−O3, and (h) Si−O4.

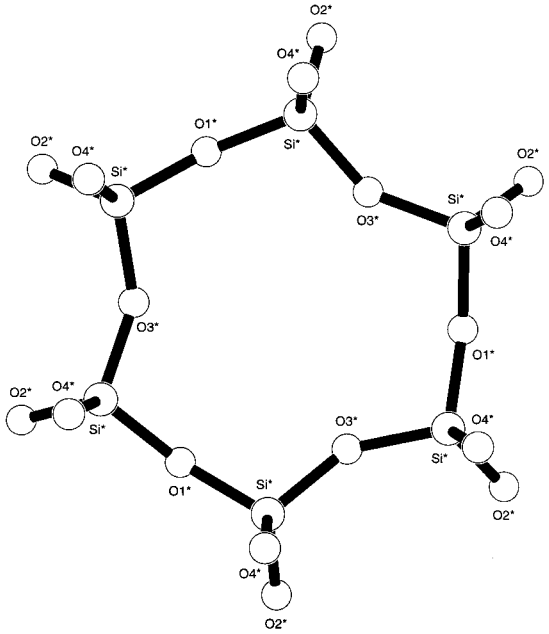

Figure 8. Representation of the single six-membered ring in chabazite viewed down the *c* axis.

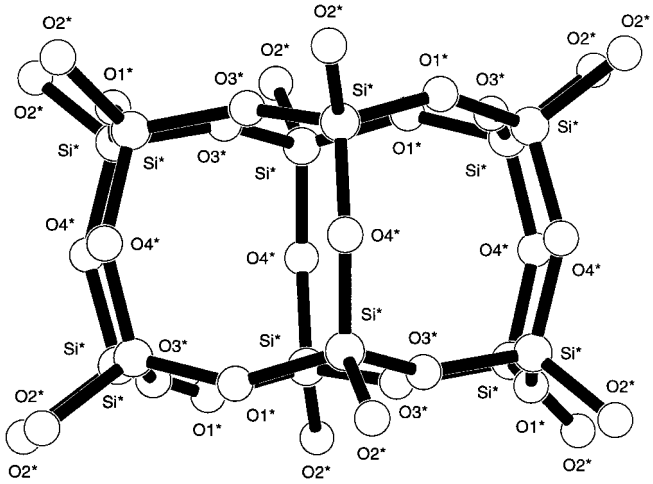

Figure 9. Representation of the double six-membered ring in chabazite viewed perpendicular to the *c* axis.

contraction of the cell depending on the template. The thermal behavior of the calcined material would be expected to be essentially independent of the template used.

Conclusions

Of the three models tested, the free isotropic refinement strategy was found to be most suitable in the case of chabazite although the data were not of sufficient quality to give an unambiguous thermal motion model. Both ITQ-4 and chabazite contract, chabazite exceptionally so with its contraction exceeding that of even AlPO-17, the most strongly contracting material known as the temperature approaches 873 K ($\alpha_v/3 = -16.7$ cf. -11.7×10^{-6} K^{-1}). Within this system the key feature appears to be the behavior of the Si−O1−Si and Si−O3−Si angles, which contract, pulling the single six-membered rings together and contracting the *a* and *b* axes. The *c* axis contracts due to a shortening of the Si−O4−Si bond pathway which bridges the double six-membered rings. Whether these effects are static or merely due to

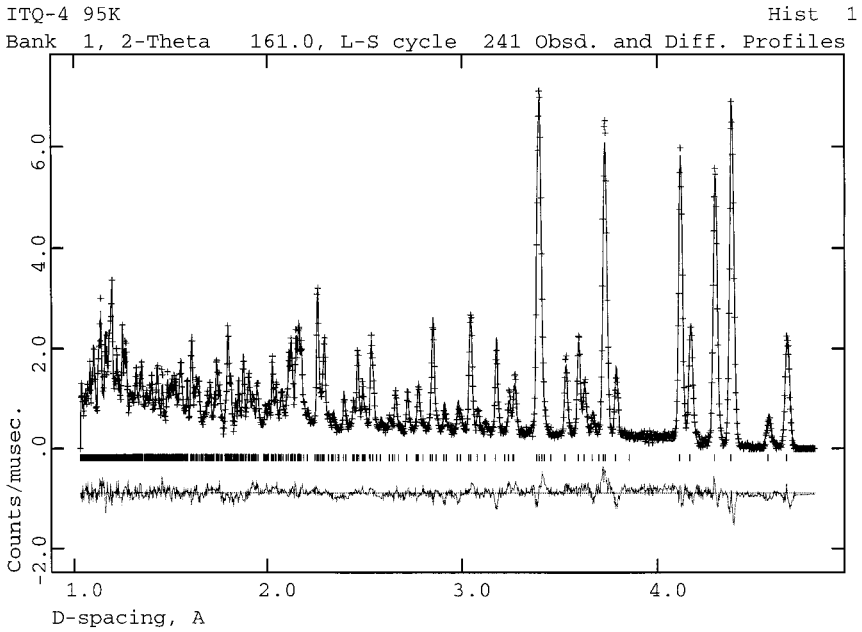

Figure 10. Typical neutron Rietveld plot for ITQ-4 at 95 K.

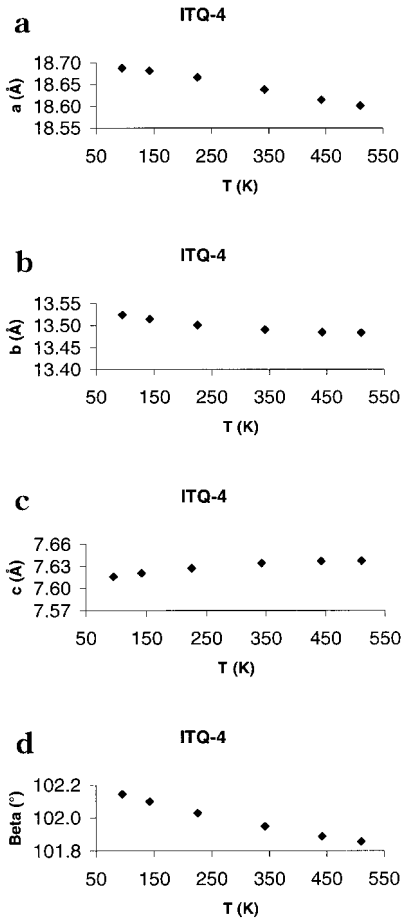

Figure 11. Plots of the evolution of unit cell parameters vs temperature for ITQ-4 for (a) the *a* axis, (b) the *b* axis, (c) the *c* axis, and (d) β angle.

transverse vibration of bridging O atoms is still an ambiguity. Higher resolution data will be required in order that a more satisfactory model of thermal motion effects can be obtained.

The relative strength of the contraction of the *c* axis in chabazite compared to that of its *a* and *b* axes is the inverse of that in AlPO-17 which showed a stronger contraction in its *a* and *b* rather than *c* axes, despite the fact that the two structures are closely related.

Table 4. Experimentally Determined Polynomial Parameters for ITQ-4

axis	p_2	p_1	p
a	0	-2.154×10^{-4}	18.712
b	2.529×10^{-7}	-2.489×10^{-4}	13.545
c	-1.310×10^{-7}	1.314×10^{-4}	7.604
vol	-1.256×10^{-5}	-9.862×10^{-3}	1882.9

Table 5. Comparison of CTEs for SSZ-42 and ITQ-4

	this work ($\times 10^{-6}$ K^{-1})	Gale[6] ($\times 10^{-6}$ K^{-1})
α_a (95 K)	−11.5	−8.5
α_a (510 K)	−11.5	−9
α_b (95 K)	−15	−2.5
α_b (510 K)	+0.66[a]	−4.5
α_c (95 K)	+14	−5
α_c (510 K)	−0.3[a]	−5
α_β (95 K)	−9.3	+3.5
α_β (510 K)	−4.3	+8

[a] Change sign at ~480 K.

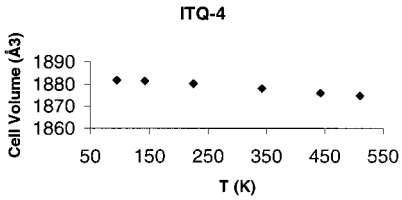

Figure 12. Plot of the evolution of unit cell volume vs temperature for ITQ-4.

The results from ITQ-4 do not show adequate precision to draw definite conclusions of the key parameters influencing its thermal contraction. A further study extended to lower d spacings is required. However the cell parameters, which are well-defined from these data, are in contrast to Gale's calculations.[6] He found a contraction of all three axes and an expansion of the monoclinic angle compared to our results which show a contraction of the *a* and *b* axes and the monoclinic angle and an expansion of the *c* axis. Clearly further work, both experimental and computational, is merited on

these, and other related microporous systems, before a fuller explanation of their behavior can be established.

Acknowledgment. We would like to thank the EPSRC for provision of a studentship to D.A.W., Dr. P. A. Wright for useful discussions and Mr. Martin J. Maple for assistance in collecting neutron data.

CM991047Q